Trans. Indian Inst. Met.
Vol.61, No. 6, December 2008, pp. 487-496

TP 2248

Calorimetric Studies And Kinetic Parameters Of Solid State Reactions In 7017 Al-Zn-Mg Alloy

K.S. Ghosh, A.K. Kumar and M.K. Mohan*
Department of Metallurgical and Materials Engineering, National Institute of Technology, Durgapur-713 209, India.
* Department of Metallurgical and Materials Engineering, National Institute of Technology, Warrangal-506 004, India.
E-mail : ksghosh2001@yahoo.co.uk

(Received 26 May 2008 ; in revised form 30 October 2008)

ABSTRACT

Differential scanning calorimetric (DSC) studies have been carried out at different heating rates to examine the solid state reactions in a 7017 Al-Zn-Mg alloy of water-quenched (WQ) state and artificial aged tempers. All the exothermic and endothermic peaks of the thermograms indicating the solid state reaction sequence have been identified and discussed. The shifting of peak temperatures of all the reactions to higher temperatures with increasing heating rates suggests that the reactions are thermally activated and kinetically controlled. The variations of hardness with aging time at an artificial aging temperature have also been studied to obtain the under-, peak- and over aged tempers. The fraction of transformation (Y), the rate of transformation (dY/dt), the transformation function f(Y) and the kinetic parameters such as activation energy (Q) and frequency factor (k_0) of the solid state reactions in the alloy have been determined by analyzing the DSC data i.e. heat flow involved with the corresponding DSC peaks. It has been found that the kinetic parameters of the solid state reactions are in good agreement with the published data.

Q(T)	Total heat effect
E	Calibration constant
$A(T)$	Area under peak between temperature T_i and T
M	mass of the sample
ϕ, $\frac{dT}{dt}$	heating rate
δq	measured heat flow
T_f	final peak temperature of transformation
Q_o	heat effect per mole
dn	number of mole precipitation / dissolution per unit mass
Y(T)	fraction transformation at temperature T
Y	volume fraction transformation
$\frac{dY}{dt}$	rate of transformation
k	rate constant
t	time
n	growth parameter
f(Y)	transformation function
R	gas constant
Q	activation energy

1. INTRODUCTION

Aluminium alloys of 7xxx series Al-Zn-Mg are widely used in aircraft and aero-vehicle structural components. These alloys provide very high strength and stiffness in their peak aged temper. The aging behaviour and the sequence of precipitation and dissolution reactions of these alloys have been studied by various methods such as hardness measurements, resistivity, calorimetry and X-ray diffraction etc.[1-5]. It is still essentially required to study the microstructural features of the alloys for better understanding and correlating the structure-property relationships. This is because the alloy system comprises a large number of metastable and stable phases associated with the development of complex microstructural conditions owing to a variety of aging treatments[4,6,7,8].

Studies have also shown that differential scanning calorimetric (DSC) technique can be used as a supplement to TEM for rapid and quantitative description of precipitate microstructures of aluminium alloys[9,10,11], although transmission electron microscopy (TEM) is an important technique. Further, considering the limitations in quantitative TEM method, i.e. susceptibility to errors and of time-consuming, calorimetric method can conveniently be utilized to study the kinetics of all types of precipitation and dissolution reactions and aging behaviour as well[12,13].

The kinetic information of precipitation and dissolution reactions of aluminium base alloys has been obtained using resistivity and differential scanning calorimetry (DSC) techniques[14-19]. Generally, resistivity measurements are used to study the kinetics under isothermal conditions and DSC in non-isothermal conditions. Youdelis and coworkers[14] using resistivity measurements studied the precipitation in Al-Cu, Al-Mg-Si, and Al-Cu-Mg alloys. Jena *et al*[15] and Gupta *et al*[16] evaluated kinetic parameters for precipitation in Al-Cu-Mg alloy from DSC thermograms. Delasi *et al*[9] assumed a first order kinetic relationship and used stepwise integration procedure to determine the rate constants for the dissolution reaction in three 7xxx series alloys. They also applied absolute reaction rate theory to find out the activation energy for various reactions. Donoso[20] estimated the activation energies for dissolution of GP zones and η′ phase in the Al-4.5 at.% Zn–1.75 at.% Mg alloy from the peak temperature which corresponds to the maximum rates of heat generation. Papazian[13] examined the kinetics of precipitation and dissolution reactions in aluminium 2219 and 7075 alloys by DSC technique. It is discussed in the literature that the kinetic parameters of the reactions were derived from the different aging tempers of T4, T6 etc. In the present investigation, the sequence of solid state reactions in a 7017 alloy and the kinetic parameters, such as activation energy (Q), frequency factor (k_0) and the transformation function

f(Y) of the precipitation and dissolution reactions have been determined by different techniques from the DSC thermograms, carried out at different heating rates, of the as-quenched and naturally aged for a short period of a 7017 alloy.

2. EXPERIMENTAL

2.1 Materials

The chemical compositions (wt. %) of the 7017 alloy is Zn - 5.95, Mg - 1.98, Cu - 0.162, Cr - 0.186, Fe- 0.35, Si – 0.082 and Al – balance. The alloy was obtained in plate form of approximate 10 mm thickness from Defence Metallurgical Research Laboratory (DMRL), Hyderabad, India. The 7017 alloy was cast, homogenized and rolled to 10 mm thickness. Specimens of dimensions 10 mm × 10 mm × 2 mm were cut from the 7017 alloy plate and was subjected to solutionising treatment at 480°C for 30 minutes, quenched in water and followed by artificial aging at temperature of 130°C upto a time period of over aged (T7) temper. Vicker's hardness tester, Model VH – 3B was used for measuring hardness to assess the aging behaviour. The load applied for measuring hardness is 10 kg and the reported value of hardness is an average of three hardness readings.

2.2 DSC studies

For DSC studies, specimens of approximately 6 mg were obtained from the as-quenched, under-aged and over-aged states. DSC runs were initiated from ambient temperature to 540°C at different heating rates in nitrogen atmosphere, using a TA instrument model Q10. Baseline correction and baseline drift are properly accounted for in order to free from parasitic effects and perfection in measuring accurate and reliable calorimetry heat evolution and absorption of the DSC unit - although the modern DSC instruments are reliable which have remarkably high accuracies in measurement. Ultra pure aluminium of more or less same mass of the test sample was used as a reference material. A calibration run on an ICTA temperature standard e.g. indium was stored in the default data area of the computer of the DSC unit. Once a DSC run of a sample was completed, the output (i.e. the heat released or absorbed corresponding to precipitation or dissolution reactions), the net heat flow to the reference relative to the samples as a function of temperature was recorded. The corrected DSC trace was obtained by accounting the baseline correction. In the DSC thermogram, the exothermic and endothermic reactions were plotted upward and downward respectively. The peak temperatures of all the peaks were noted.

3. RESULTS AND DISCUSSION

3.1 Artificial aging behaviour

Figure 1 shows the variation of hardness with aging time of the solutionised and water quenched samples artificially aged at temperature 130°C. The Fig.1 exhibits the characteristic aging behaviour of a precipitation hardenable aluminium base alloys, i.e. an increase of hardness, attainment of maximum peak hardness (peak aged temper) followed by decrease of hardness (over aged temper) with increasing aging time. This variation of hardness with aging time could be attributed to

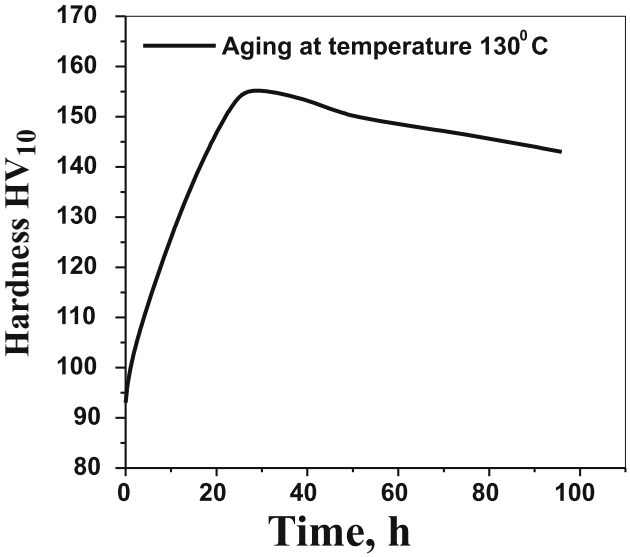

Fig. 1 : Variation of hardness with aging time of the 7017 alloy for artificial aging at temperature 130°C

the formation of GP zones, precipitations of matrix strengthening semi-coherent η′ ($MgZn_2$) phase and formation and growth of incoherent equilibrium η ($MgZn_2$) phase[1,8,21].

3.2 DSC thermograms of solution treated water quenched state

Figure 2 shows the DSC thermograms of solution treated, water quenched and naturally aged for approximately 3 hours of the 7017 alloy at the heating rates of 10, 15, 20 and 30°C/min. The curves are smoothened with the help of built-in software in the computer controlled DSC unit.

In the case of age hardenable aluminum alloys, normally the formation of precipitates is an exothermic process whilst their dissolution is an endothermic process[22]. The peak temperature for the precipitation represents the temperature at which the two factors i.e. the fall of the driving forces for

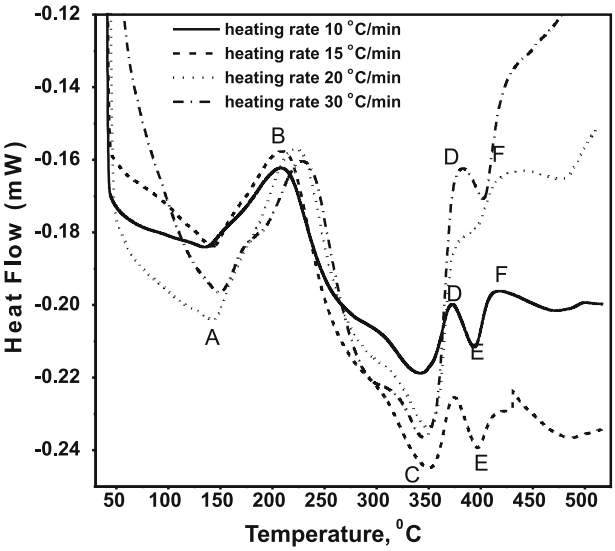

Fig. 2 : DSC thermograms of solution treated, water quenched and natural aged for 3 hours 7017 alloy at different heating rates.

the continued precipitation (i.e. the decrease of supersaturation with the rise of temperature during DSC run) and the increase of diffusivity with the increase of temperature competing and resulting maximum precipitation rate.

The DSC thermograms (Fig. 2) exhibiting exothermic and endothermic peaks indicates the sequence of precipitation and dissolution reactions in the alloy as follows,

Super saturated solid solution (SSSS) $\alpha \rightarrow GP \rightarrow \eta' \rightarrow \eta$ ($MgZn_2$)

But, in the process, there may be overlap of one transformation with another, and hence the peaks in the DSC thermograms are overlapped by one another. The different peaks in the thermograms marked with alphabets A-F could be identified as: *A* – dissolution of Guinier–Preston (GP) zones, *B* - precipitation of η' ($MgZn_2$) phase, *C* – dissolution of η' ($MgZn_2$) precipitates, *D* – precipitation of equilibrium η ($MgZn_2$) phase, E – dissolution of η and F – surface oxidation. The precipitation sequence for the 7xxx series alloys and the peak temperatures of all the peaks with different heating rates (given in Table 1) are in agreement with the literature[3,9,10,13,23,24]. The GP zones are coherent with the matrix; the semi-coherent intermediate η' ($MgZn_2$) phase has been described as having monoclinic unit cell while the incoherent equilibrium η ($MgZn_2$) phase is hexagonal[8,9] .

In precipitation hardenable aluminium base alloys, the formation of GP zones commences from the room temperature itself and this is enhanced due to the introduction of dislocations while obtaining (by shearing and/or punching) the DSC samples. It is also reported in literature that there are two types of GP zones in Al-Zn-Mg based alloys, which are solute rich GP 1 zones, or Mg/Zn cluster; and solute/vacancy-rich GP II zones. While heating the sample during the DSC run, the dissolution of already formed GP zones take place which is reflected in the endothermic peak A in Fig. 2. The dissolution peak temperature is in agreement with reported dissolution temperature range of 50–150°C [17]. The exothermic peak region B is associated with the precipitation of semi-coherent η' phase.

Further, from the Fig. 2, in general, it can be mentioned that the peak temperatures of the peaks have shifted to higher temperatures with the increasing heating rates, of course, with an exception at some heating rates for peak C and D which might have happened due to the occurrence of the reactions for these peaks at very close temperature ranges and /or overlapping of these reactions. Thus, the shifting of the precipitation and dissolution reactions with heating rates are thermally activated and kinetically controlled[13,15,25-28]. The peak temperatures for these solid state reactions at different heating rates are given in Table 1.

3.3 Thermograms of under- and over aged tempers

Figure 3 shows the DSC thermograms of the 7017 alloy of under aged and over aged tempers. The thermogram of the over-aged temper of the alloy exhibits two clearly endothermic peaks at temperatures 221°C and 335°C. The absence of exothermic peak is due to the fact that the solid solution is not super saturated with solutes atoms; in other words, the alloy temper contains equivalent amounts of semi-coherent matrix strengthening η' phase and equilibrium η phase. But, the thermogram of the under-aged temper shows a small exothermic peak B, endothermic peaks A and C. The appearance of peak B in the under-aged alloy indicates that the solid solution is still super saturated with the solutes i.e. the alloy temper does not contain equivalent amounts of η' phase. Thus, the presence of the exothermic peak B in the

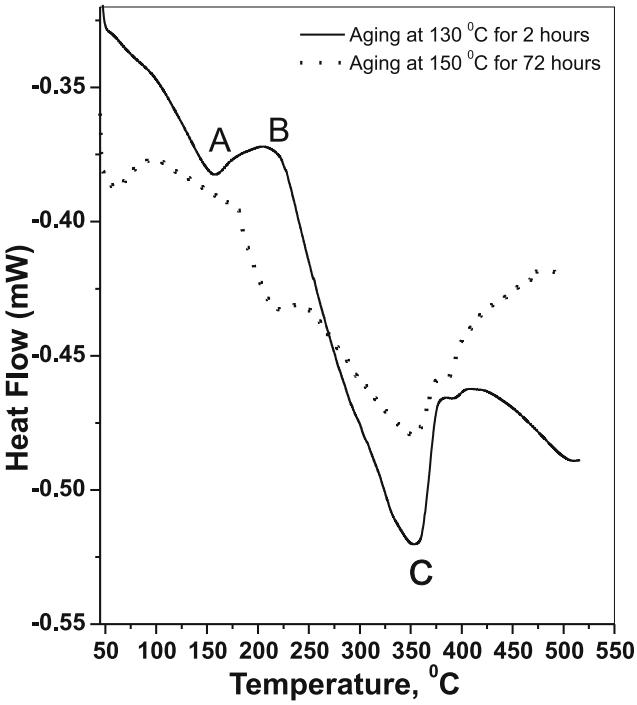

Fig. 3 : DSC thermograms of 7017 alloy of under aged and over aged tempers at the heating rate of 10°C/min.

Table 1

Peak temperatures of the DSC peaks of the as-quenched of the 7017 Al-Zn-Mg alloy at different heating rates.

Alloy	Heating rate, °C / min	Peak A T_p	Peak B T_p	Peak C T_p	Peak D T_p	Peak E T_p
7017	10	134	208	342	392	415
	15	142	209	340	396	430
	20	143	222	349	402	435
	30	148	228	346	397	500

T_p is the peak temperature.

thermogram, indicating the precipitation of η′ phase and growth of the existing η′ phase as well, is obvious. Similar observations, in the DSC studies of Al-Li-Cu-Mg-Zr alloys of under-aged and retrogressed tempers, have also been reported in literature[28]. Further, it is to be noticed that the area under the peak region A for the thermogram of under-aged temper (Fig. 3) is less than the area under the peak region A in Fig. 2. This is because the amounts of precipitation of η′ phase during DSC run is more for the solution treated and water quenched state than to that of under-aged temper. This confirms that the under-aged temper contains a certain amounts of matrix strengthening η′ phase. This is reflected in the aging behaviour (Fig. 1) as there is an increase of hardness with aging time upto peak aged temper.

3.4 Analysis of DSC data

In the DSC run, the total heat effects, Q(T), observed between the initial temperature of a peak T_i and at a temperature T, is given by

$$Q(T) = \frac{EA(T)}{M\phi} \tag{1}$$

Where M is the mass of the sample, ϕ is the heating rate, E is (calibration) constant and A(T) is the area under the peak between temperatures T_i and T, which is the observed heat flow that is associated with the precipitation and dissolution reactions[15,16,19]. A(T) can be expressed as

$$A(T) = \int_{T_i}^{T} (\delta q)\, dT \tag{2}$$

where, δq is the measured heat flow, involved for the specific precipitation or dissolution reactions, to the inert reference (high purity annealed aluminum) relative to the sample as a function of temperature at a constant heating rate ϕ.

If T_f is the final temperature of the peak

$$Q(T_f) = \frac{EA(T_f)}{M\phi} \tag{3}$$

If Q_0, is the heat effect per mole of precipitate, then the heat effect is dQ given by

$$dQ = Q_o\, dn \tag{4}$$

where, dn in the number of moles of precipitate which form or dissolve per unit mass of the alloy.

Integrating equation (4) and substituting in equation (1), we obtain

$$n(T) = \frac{EA(T)}{Q_0 M\phi} \tag{5}$$

and

$$n(T_f) = \frac{EA(T_f)}{Q_0 M\phi} \tag{6}$$

Thus, the fraction of the precipitation Y(T) at temperature T, can be expressed as

$$Y(T) = \frac{n(T)}{n(T_f)} \tag{7}$$

Therefore, from equation from (5), (6) and (7)

$$Y(T) = \frac{A(T)}{A(T_f)} \tag{8}$$

From the DSC thermograms, the fraction transformed Y(T) i.e. the amounts of phase precipitated or dissolved at a given temperature range, can be expressed according to equation (8) and is illustrated schematically in Fig. 4.

The rate of transformation can be written

$$\frac{dY}{dt} = \frac{dY}{dT} \cdot \frac{dT}{dt}$$

Thus,

$$\frac{dY}{dt} = \frac{dY}{dT} \cdot \phi \tag{9}$$

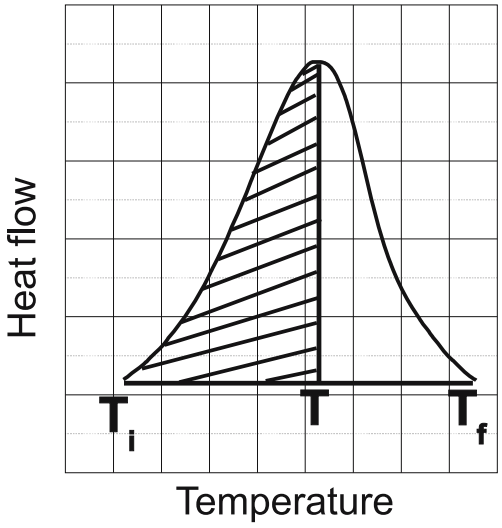

Fig. 4 : Shaded area shows the fraction transformation within the temperature range T_1 to T_f.

3.5 Non-isothermal transformation

For complex transformation and precipitation reactions, the reaction kinetics for non-isothermal transformation are usually expressed[19], according modified Avrami-Johnson-Mehl equation, in the form of

$$Y = 1 - \exp(-k^n t^n) \tag{10}$$

where $k = k_0 \exp(-Q/RT)$ (11)

Where Y is the volume fraction of precipitation at time t, and *k* is the rate constant and n is the growth parameter, which depend on the nuclei density and precipitate growth modes, respectively. Q and R are the activation energy of the reaction and gas constant, respectively. The kinetic equation (10) is considered to be accurate based on the assumptions that (i) the product phase are randomly distributed, (ii) nuclei are randomly distributed, (iii) average growth rates are independent of position in the sample, (iv) impingement on objects other than neighbouring domains of the product phase is negligible and (v) blocking resulting from anisotropic growth is negligible.

The logarithmic form of equation (10) yields

$$\log \ln[1/(1-Y)] = n \log t + n \log k \quad (12)$$

The rate constant, k and the growth parameter, n are the constants for a process mechanism. Therefore, for a specific value of *n*, the term *n log k* in equation (12) remains constant. The plot of log ln [1/(1-Y)] vs. log *t* of the equation (12) yields a straight line function, from which the value of n(slope) and k(from the intercept) can be obtained.

For non-isothermal transformation, it is more expedient to use equation (10) in developing transformation rate and related expression. The rate of transformation can be expressed as

$$\frac{dY}{dt} = k(T) f(y) \quad (13)$$

where f(Y) is the implicit function of Y from equation (10).

Combining with equation (13) and the derivative of equation (10) results

$$f(Y) = n(1-Y)[-\ln(1-Y)]^{(n-1)/n} \quad (14)$$

The non-isothermal kinetic data stated in the DSC analysis in equation (9) can be written as

$$\frac{dY}{dT} = \frac{1}{\phi}.\frac{dY}{dt} = \frac{1}{\phi} \cdot k(T) f(Y) \quad (15)$$

Substituting k(t) from equation (11) into equation (15) and taking logarithm and rearranging, the equation (19) simplifies as

$$\ln[(dY/dT)_Y \phi] = \ln[f(Y) k_0] - (Q/R)(1/T) \quad (16)$$

If for a heating rate ϕ_j, the temperature at which a constant fraction (Y′) of precipitate is obtained, T_j is then,

$$\ln[(dY/dT)_{Y'} \phi_j] = \ln[f(Y') k_0] - (Q/R)(1/T_j) \quad (17)$$

where ϕ_j is the j^{th} heating rate, $(dY/dT)_{Y'}$ is the rate at a given fraction of transformation (Y′), and is the T_j temperature at which the fraction is (Y′) at heating rate ϕ_j. Therefore, a plot of $\ln[(dY/dT)_{Y'} \phi_j]$ vs. $(1/T_j)$, under different heating rates, will give a straight line of slope (-Q/R) from which the value of activation energy Q can be determined.

3.6 Kinetic parameters of solid state reactions in 7017 alloy

3.6.1 Dissolution of GP zones - Peak A

The exothermic DSC peak A (GP zones) for the water-quenched 7017 alloy at different heating rates is shown separately in Fig. 5a. From these curves, the precipitate amount (volume fraction, *Y*) and precipitate rate (*dY/dt*) can be calculated from equation (8) and equation (9) respectively. The plot of *Y* and the precipitation rate (*dY/dt*) are shown as a function of temperatures in Fig. 5b and Fig. 5c respectively. The Y vs. T curve is sigmoidal in shape and shift to higher temperatures with the increase of heating rate. The variation of rate of transformation with temperatures is typical of a sigmoidal *Y* - *T* curve. Further, there are also considerable shifts in the maxima of the rate of transformation curves (Fig. 5c) to the higher temperatures with increasing heating rates. It implies that the transformation is thermally activated and kinetically controlled.

The data obtained from the Fig. 5c are plotted according to equation (17) in Fig. 5d for three values of fraction transformed, Y′ 0.25, 0.50 and 0.75. The slopes of the three linear straight lines give the average value, 71.8 +/- 10.7 kJ/mol as the activation energy (Q) for the process. The activation energy value for the dissolution of GP zones is in good agreement with the value obtained by others[9,10,13,29]. For comparison, Table 2 gives the kinetic parameter values which are evaluated by the author for the 7017 alloy and those reported in literature for the 7xxx series alloys of different tempers.

It is to be mentioned that the calculated Q has to be taken as apparent activation energy since, in many cases, the processes involved are not unique and also not precisely definable. Furthermore, due to complexity of the precipitation and dissolution reactions phenomena involved that results in an overlap of their effects in the DSC peaks of 7017 Al-Zn-Mg alloy, the energy content associated with a particular process (precipitation or dissolution) cannot be determined accurately. As a consequence the determination of enthalpy effects may result some erroneous value. Notwithstanding the above restrictions, meaningful values of Q associated with distinguishable processes may be obtained since the temperature (T) value at the signal peak is little affected by the uncertainty of the baseline[30] .

In order to assess the progress of reactions at all temperatures and for all temperature – time programmes, the function f(Y), the constants, k_0 and Q is required to be determined. In general, the reaction function f(Y), is unknown at the outset of the analysis. A range of standard functions which represent particular idealized reaction models have been proposed[31-32]. The function f(Y) is determined by assuming suitable forms and using experimental data to verify. Reactions that occur by nucleation and growth yield sigmoidal behaviour. A general relationship[33] that gives sigmoidal behaviour is

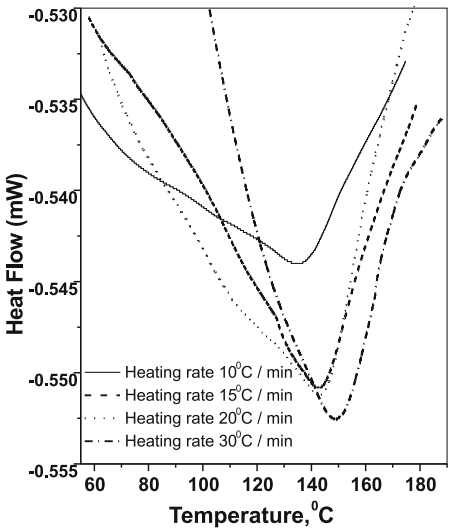

Fig. 5a : Dissolution Peaks of GP zones of the as-quenched 7017 alloy at different heating rates.

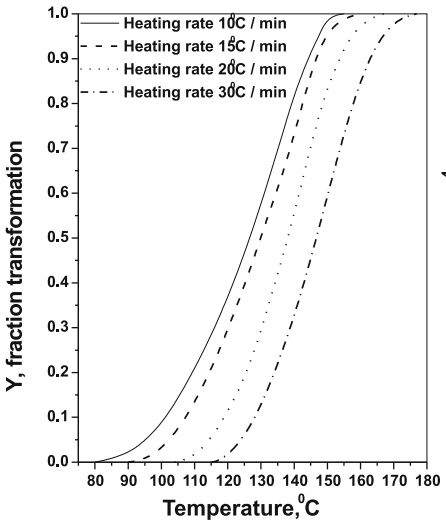

Fig. 5b : Plot of Y vs. T of peak A of DSC thermogram of the 7017 alloy.

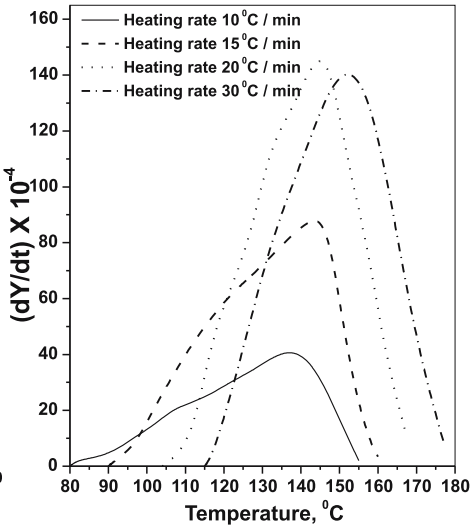

Fig. 5c : Plot of (dY/dt) x 10^{-4} vs. T of peak A of DSC theogram of 7017 alloy.

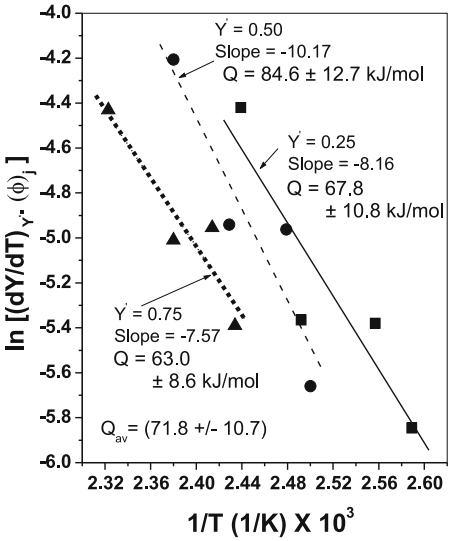

Fig. 5d : Plot for the determination of activation energy for GP zones dissolution of the 7017 alloy after equation (17).

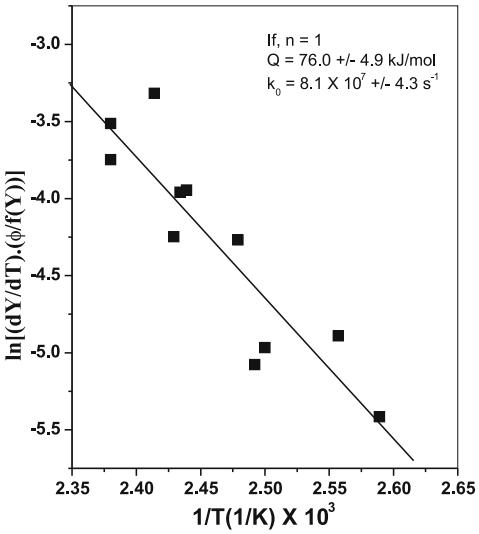

Fig. 5e : Plot after equation (24) for determining the transformation function f(Y) of GP zones dissolution in the 7017 alloy.

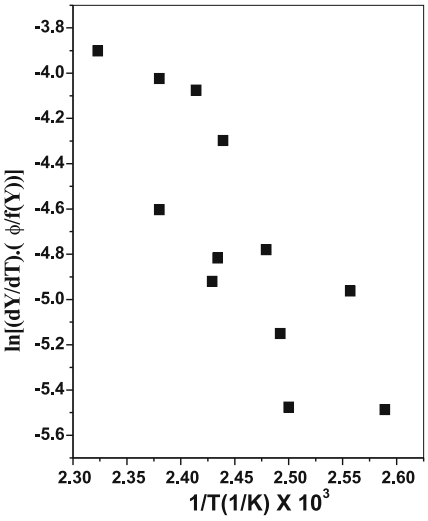

Fig. 5f : Plot after equation (21) for the dissolution of GP zones in the 7017 alloy.

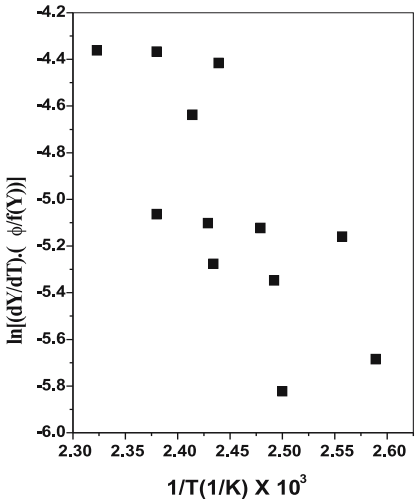

Fig. 5g : Plot after equation (22), for the dissolution of GP zones in the 7017 alloy.

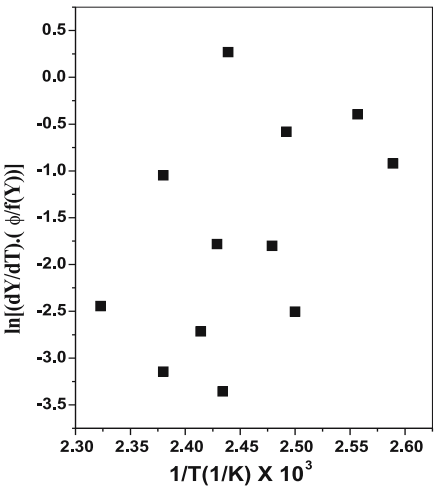

Fig. 5h : Plot after equation (23), for the dissolution of GP zones in the 7017 alloy.

$$f(Y) = Y^r (1\text{-}Y)^m \quad (18)$$

where exponents r and m are constant. The formalism can incorporate Johnson-Mehl-Avrami-Kolmogorov [JMAK] kinetics and the form that also yield sigmoidal behavior is

$$f(Y) = n[-\ln(1-Y)]^{(n-1)/n}(1-Y) \quad (19)$$

Where the exponent *n*, growth parameter, is a constant which depends on precipitate growth modes. If, *n* is considered to be 1, 2 and 3 [32,34] , the equation (19) reduces to equations (20), (21) and (22) respectively, as expressed below

$$f(Y) = (1-Y) \quad (20)$$

$$f(Y) = 2[-\ln(1-Y)]^{1/2}(1-Y) \quad (21)$$

$$f(Y) = 3[-\ln(1-Y)]^{2/3}(1-Y) \quad (22)$$

Further, for a three-dimensional diffusion equation, the transformation function f(Y) may also be expressed as [16]

$$f(Y) = [1 - (1\text{-}Y)^{1/3}]^2 \quad (23)$$

Plots are made to verify the validity of the above expressions in equations (20) to (23), for the dissolution of GP zones. But, the transformation function f(Y) according to the relationship (20) is most satisfactory, as shown in Fig. 5e, whereas the other relationships after equations (21), (22) and (23) are unsatisfactory i.e. data are more scattered, as shown in Fig. 5f, 5g and 5h, respectively.

Now, combining equations (9), (16) and (20) yields

$$\ln[(dY/dT)(\frac{\phi}{1-Y})] = \ln k_0 - \left(\frac{Q}{R}\right)\left(\frac{1}{T}\right) \quad (24)$$

The activation energy for the dissolution of GP zones in the 7017 alloy after equation (24) is found to be 76.0 +/- 4.9 kJ/mol and k_0 is found to be 8.1 X 10^7+/-4.3s^{-1}. The activation energy values obtained after equations (17) and (24) are in close match. Thus, the best transformation function f(Y) describes the dissolution of GP zones in the 7017 alloy is (1 - Y).

3.6.2 Precipitation of η′ ($MgZn_2$) phase – peak B

The peak B for the precipitation of η′ phase (DSC thermograms in Fig. 2) is shown separately in Fig. 6a. From these curves, the fraction of precipitation, *Y* and the precipitate rate (*dY/dt*) are calculated from equation (8) and equation (9). Figs 6b and 6c exhibit the plot of *Y* vs. T and (*dY/dt*) vs. T, respectively. Likewise the dissolution of GP zones, the Y vs. T curves are sigmoidal in shape and have shifted to higher temperatures with the increase of heating rate. The variation of rate of transformation with temperatures is typical of a sigmoidal *Y* - *T* curve. There are also considerable shifts in the maxima of the rate of transformation curves to the higher temperatures with the increasing heating rates, implies that the transformation is kinetically controlled.

The data obtained from the Fig. 6c are plotted according to equation (17) in Fig. 6d for three values of fraction transformed, Y′ 0.25, 0.50 and 0.75. The slopes of the three linear straight lines give the average value 62.1 +/- 8.9 kJ/mol as the activation energy (Q) for the precipitation of η′ phase. The activation energy value is in good agreement with the value reported in literature for 7xxx series alloys[9,10,13,29] .

Likewise for the dissolution of GP zones, plots are made to determine the transformation function, for the precipitation of η′ ($MgZn_2$) phase, after combining equations (9) and (16) with equations (20) to (23). But, the relationship (20) is most

Table 2

Kinetic parameters for solid state reactions in the 7017 alloy studied and values available in the literature.

Alloy Studied / From literature	Peak Nature of peak	A GP zones dissolution	B η′ precipitation
7017	Q (kJ/mol)(after equ. (17))	71.8 +/- 10.7	62.1 +/- 8.9
	Q (kJ/mol) (after equ. (24))	76.0 +/- 4.9	70.7 +/- 4.5
	k_0 (s^{-1})	8.1 X 10^7 +/- 4.3	7.0 X 10^5 +/- 3.5
	f(Y)	(1-Y)	(1-Y)
(From Literature) Al-Zn-Mg-Cu-Li	Q (kJ/mol)	100 +/- 6.4	—
(Ref 29)	k_0 (min^{-1})	7.18 X 10^{11}	—
7075-T651 temper	Q (kJ/mol)	107.4 +/- 6.7	66.5 +/- 4.2
7075-T7351 temper (Ref 9)	Q (kJ/mol)	86.1 +/- 7.2	63.1 +/- 5.4
7449-T6 *(Ref. N Kamp, PhD thesis, Univ of Southampton, 2002)*	Q (kJ/mol)		70 +/- 7
Al-5.1Mg-2.35Zn-2.0Cu– T6 temper(Ref: C. Garber-Cordovilla & E. Louis; Met Trans A; 1990 2277)	Q (kJ/mol) k_0 (s^{-1}) 69.2 5.0×10^6	—	

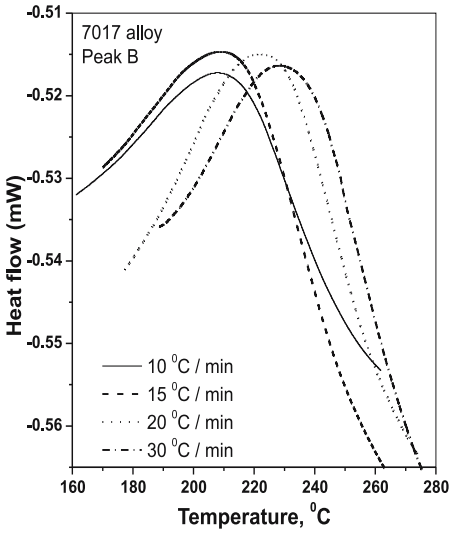

Fig. 6a : Precipitation of η′ phase peak of the as-quenched 7017 alloy at different heated rates

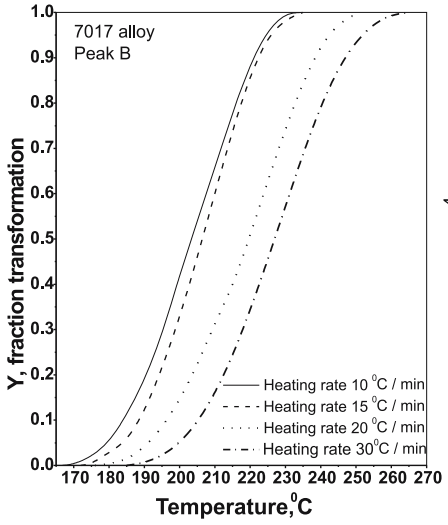

Fig. 6b : Plot o Y vs. T of peak B of DSC theogram of 7017 alloy.

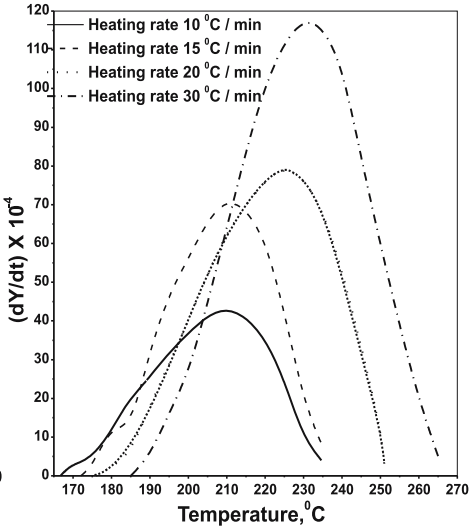

Fig. 6c : Plot of (dY/dT) x 10-4 vs. T of peak B of DSC theogram of 7017 alloy.

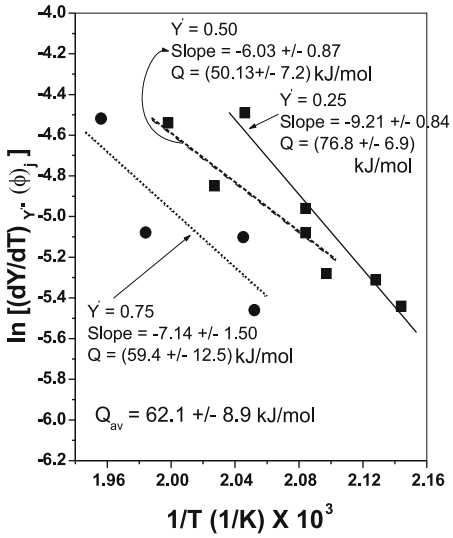

Fig. 6d : Plot for the determination of activation energy for the precipitation of η′ phase of the 7017 alloy after equation (17).

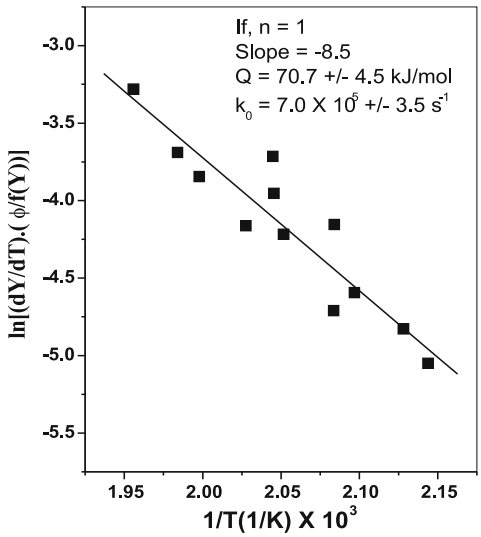

Fig. 6e : Plot after equation (24) of the precitpitation of η′ phase in the 7017 alloy.

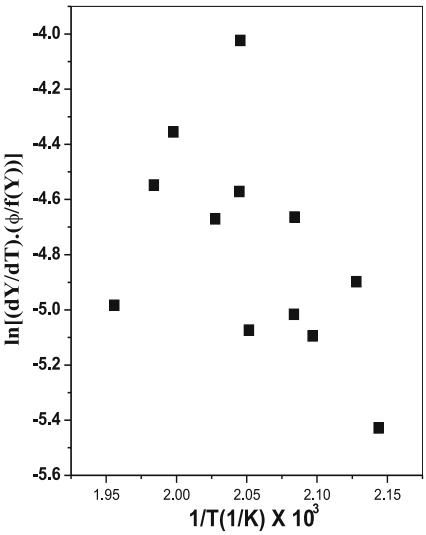

Fig. 6f : Plot after equation (21) of the precitpitation of η′ phase in the 7017 alloy.

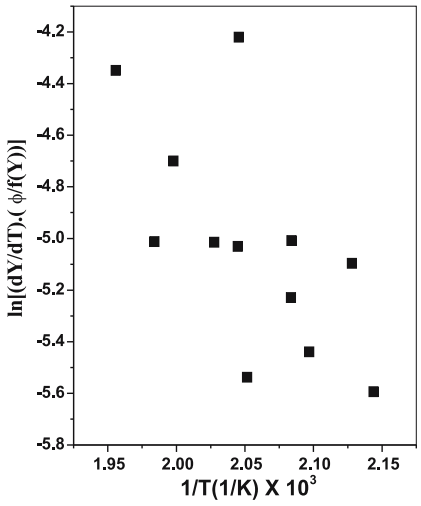

Fig. 6g : Plot after equation (22) of the precitpitation of η′ phase in the 7017 alloy.

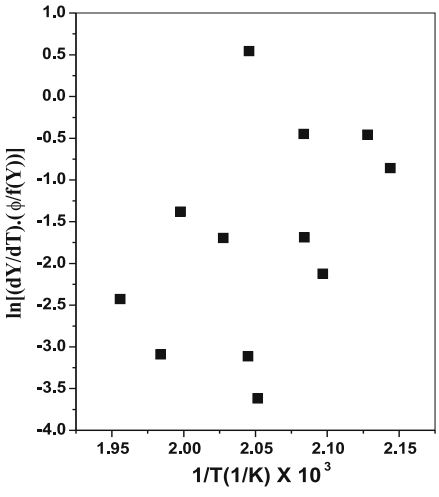

Fig. 6h : Plot after equation (23) of the precitpitation of η′ phase in the 7017 alloy.

satisfactory, as shown in Fig. 6e, whereas the other relationships after equations (21), (22) and (23) are unsatisfactory, as shown in Fig. 6f, 6g and 6h, respectively i.e. data are more scattered and best linear fit is not possible to obtain activation energy for the reaction.

The activation energy for the precipitation of η′ phase in the 7017 alloy after equation (24) is found to be 70.7 +/- 4.5 kJ/mol and k_0 is found to be 7.0 X 10^5+/-3.5s^{-1}. The activation energy values obtained after equations (17) and (24) are in close match. Thus, the best transformation function f(Y) describes the precipitation of η′ phase in the 7017 alloy is (1 - Y). This agrees that the η′ phase precipitates form by diffusion controlled parabolic growth or diffusion controlled linear axial growth which is expected to satisfy the Johnson-Mehl type expression where the value of coefficient, *n* is equal to one.

3.6.3 Dissolution of η′ ($MgZn_2$) phase and precipitation of η phase – peaks C and D

From the present DSC thermograms (Fig. 2) using the techniques discussed in the previous sections, attempts have not been made to determine the kinetic parameters and the transformation functions for the dissolution of η′ ($MgZn_2$) phase (peak C) and precipitation of η phase (peak D) reactions, as the determined values of kinetic parameters for either of the reactions will not be accurate and appropriate. This is because the calculation of fraction transformation after equation (8) will not at all be correct for either of the processes, as the peaks C and D of the thermograms are very close within a small temperature range, which is an indication of a large degree of overlapping of dissolution of η′ ($MgZn_2$) phase and the precipitation of η phase reactions.

4. CONCLUSIONS

- The DSC thermograms of the 7017 alloy taken at different heating rates have exhibited many endothermic and exothermic peaks which represent the sequence of precipitation and dissolution reactions such as the formation of GP zones, the precipitation of η′ phase, the dissolution of η′ phase, and the precipitation of η′ phase etc. The comparison of DSC thermograms of over-aged and under-aged tempers indicate the fact that the over-aged temper contains equivalent amounts of semi-coherent matrix strengthening η′ phase and equilibrium η phase, whereas, the solid solution of under-aged temper (exhibiting a small exothermic peak B) is still super saturated with the solutes. Further, the shifting of the reaction peaks at higher temperatures with increasing heating rates imply the reactions are thermally activated and kinetically controlled processes.

- From the DSC data, the technique to determine the fractional transformation Y, the method to determine activation energy (Q), frequency factor (k_o) and the transformation function f(Y), have been discussed.

- The activation energy Q, frequency factor k_0 and the function f(Y) of the rate equation for the dissolution of GP zones in the 7017 are found to be 76.0 +/- 4.9 kJ/mol, 8.1 X 10^7 +/- 4.3 s^{-1} and (1-Y), respectively.

- The activation energies Q and frequency factor k_0 of the exothermic peak B for the precipitation of η′ phase in the 7017 alloy are found to be 70.7 +/- 4.5 kJ/mol and 7.0 X 10^5 +/- 3.5 s^{-1}, respectively. The transformation function that best describes the precipitation of η′ phase is (1-Y). This agrees that the η′ phase precipitates form by diffusion controlled parabolic growth which is expected to satisfy the Johnson-Mehl type expression where the value of coefficient, *n* is equal to one.

- From the present DSC thermograms, it is not possible to determine the kinetic parameters accurately for the dissolution of η′ phase and the precipitation of η phase as there is complete overlapping within a small temperature range for these transformations.

ACKNOWLEDGEMENT

The authors would like to thank Dr. G. Madhusudhan Reddy, Scientist, Defence Metallurgical Research Laboratory (DMRL), Hyderabad, India for providing the alloy and Mr. M.N. Roy, Assistant Professor, Department of Metallurgical and Materials Engineering, National Institute of Technology, Durgapur for his valuable suggestions.

REFERENCES

1. Polmear I J, *J. Inst. Met,* **86** (1958-59) 24 and 113.
2. Hirano K and Iwasakai H, *Trans Jpn Inst of Metal*, **5** (1964) 162.
3. Park J K and Ardell A J, *Mater Sci. and Engg.,* **A114** (1989) 197.
4. Danh N C, Rajan K and Wallace W, *Metal Trans A*, **14A** (1983) 1843.
5. Deschamps A, Livet F and Brechet Y, *Acta Mater,* **47** (1998) 281.
6. Rajan K, Wallace W, Beddoes J C, *J of Materials Science*, **17** (1982) 2817.
7. Kanno M, Araki I and Cui Q, *Mater Sci and Tech,* **10** (1994) 599.
8. Mondolfo I F, *Metals Mater,* **5** (1971) 95.
9. Delasi R J and Adler P N, *Metal Trans A*, **8A** (1977) 1177.
10. Adler P N and Delasi R J, *Metal Trans A,* **8A** (1977) 1185.
11. Papazian J M, *Metal Trans A,* **12A** (1981) 269.
12. Papazian J M, Delasi R J and Adler P N Adler, *Metal Trans A,* **11A** (1980) 135.
13. Papazian J M, *Metal Trans A,* **13A** (1982) 761.
14. Youdelis W V and Fang W, *Sci and Engg of Light Metals*, (edited by K Hirano, H. Oikawa and K. Ikeda), *Japan Inst of Light Metals,* Tokyo, (1991) 917.
15. Jena A K, Gupta A K and Chaturvedi M C, *Acta Metal*, **37** (1989) 885.
16. Gupta A K, Jena A K, and Chaturvedi M C, *Scripta Met.,* **22** (1988) 369.
17. Lloyd D J and Chaturvedi M C, *J. Mater. Sci.*, **17** (1982) 1819.
18. Balmuth E S, *Scripta Met,* **18** (1984) 301.
19. Luo A, Lloyd D J, Gupta A and Youdelis W V, *Acta Metal Mater*, **41** (1993) 769.
20. Donoso E, *Mater Sci Engg.,* **74** (1985) 39.
21. Kelly A and Nicholson R. B, *Progr Mater Sci.*, **10** (1963) 216.
22. Mukhopadhyay A K, Tite C N J, Flower H M, Gregson P. J. and Sale F, in 4th Int. Conf. Proc. on Aluminum-Lithium Alloys IV, (eds.) G. Champier, B. Dubost, D. Miannay and L. Sabetay), *J de Phyique, Suppl.* **48** (1987) C3:439.
23. Berg L K, Gjonnes J, Hansen V, *Acta Mater*, **49** (2001) 3443.
24. Kamp N, Sinclair I and Starink M J, *Metal Mater Trans A*, **33A** (2002) 1125

25. Starink M J, Hobson A L, Gregson P J, *Scripta Met.*, **31** (1994) 1711.
26. Starink M J and Gregson P J, *Scripta Met.*, **32** (1995) 893.
27. Starink M J and Gregson P J, *Mater Sci Forum*, **217-222** (1996) 673.
28. Ghosh K S, Das K and Chatterjee U K, *J. of Mater. Sci.*, **42** (2007) 4276.
29. Wei F, Zhao Z K, Liu P Y and Zhou T T, *Materials Forum,* **28** (2004) 75.
30. Abis S, Evangelista E, Mengucci P and Riontino G, in 5th Int. Conf. Proc. on Aluminium Lithium Alloys, (eds.) Sanders T H Jr., and Starke E A Jr.,) MCEP, Williamsburg, Virginia, (1989) 681.
31. Vyazovkin S and Wright C A, *Int. Rev. Phys Chem*, **17** (1998) 407.
32. Galwey A K and Brown M E, in Handbook of Thermal analysis and Calorimetry, edited by M E Brown, Amsterdam, Elsevier, **1** (1998) 147.
33. Sestak J, Satava V and Wendlant W W, *Thermochemica Acta,* **7** (1973) 447.
34. Starink M J, *Int. Mater. Rev,* **49** (2004) 191.